Surface rheology and Morphology of Air-Water interfaces with adsorbed layers of Beer proteins and Isohumulones

Bobae Choi

LUNDS UNIVERSITET

Department of Food Technology and Nutrition

Msc Thesis

Department of Food Technology and Nutrition
Lund University
Box 118
SE-221 00 LUND
Sweden

Printed in Sweden
Lund 2018

Abstract

A good head of beer gives nice texture and prevents releasing of aroma. The beer foam stability depends on numerous parameters. In this study, it was focused on the interfacial rheological properties such as surface tension and dilational modulus in relation the film formation by isohumulones and beer proteins at the air-water interfaces. The isohumulones and beer protein samples were prepared individually from polaris pellet and barley malt. Both isohumulones and proteins are surface active and the combination of them have even more enhanced properties. The adsorbed layer formed by only isohumulone, pre-mixed solution of proteins and isohumulones and proteins with the sequential addition of isohumulones. Thus, it can be concluded that the properties of the surface film depends on the composition and of the addition sequence of the components. The simultaneously mixed solution forms a layer with evenly distributed components over the surface and it accounts for the exceptionally high surface activity and rigidity

Acknowledgements

First of all, I am deeply grateful to my supervisor and co-supervisor, Yi Lu and Björn Bergenståhl for all their efforts, patience and encouragement. Without them, it must be even more difficult to deal with the problems that I had. I especially appreciate countless discussions we had about the results and it was genuinely helpful to develop and narrow down the idea I have. Thank you again. I am also thankful to my examiner, Lars Nilsson and professor from Physical chemistry, Tommy Nylander for allowing me to use their laboratory equipment.

Second, I would like to thank my family who support me study in Lund and always take care of me in many ways.

Third, thank you for my friends in Lund. I was happy to study together with such great classmates, especially, Imelda, Yasmin, Pim, Uli, Tawanda, Chandana, Panos and Amanda for struggling together during the thesis period. It was fun to share the office with Atma and Shuai. I want to thank Nabilah for introducing me people in our department as well. I am glad that I have met nice Korean friends there, Yeonjin, Haisol, Narae, Suyoung, Yunjeong and Taein. Special thanks to Yingdi & Rasmus and Kei & Jeanna for inviting me to your place and offering proper meals.

Fourth, I would like to express my gratitude to Federico Gomez and Cecilia Nilsson for their help to solve my problems with visa.

Last but not least, I am happy that I can finish my studies with a fruitful material. Although my thesis is not perfect, I am still proud of myself that I finalized it. It was pleasure to study at Lund University.

Contents

1. Introduction

1.1 Background and Aim

Beer foam quality is of great interest for consumers because they regard a beer with a good head as a sign of freshness. The quality of beer foam can be divided into stability, lacing and creaminess (Bamforth, 1985). The main quality addressed in this work is the beer foam stability. It is well known that proteins and isohumulone play an important role for the foam stability by foam analysis methods such as the cylinder pour test (Evans et al., 2008). It is generally suggested that foam stability is obtained through the creation of an interfacial film with firm rheology (Dickinson, 1992).

The aim of the study is to describe the properties of the surface films formed by beer proteins and hop acids. It is assumed that the properties of the films are reflected in the surface tension, surface rheology and in the surface morphology. Thus, it was investigated how beer proteins and isohumulones influence these properties independently and collectively using drop tensiometry and Brewster Angle Microscopy (BAM). It is advantageous to use BAM for studying adsorbed layers at interfaces because the microscopic observations of monolayers could be performed *in situ* (Moore et al., 1986).

2. Theory

2.1 Surface active molecules in Beer

Beer contains various components such as ethanol, proteins, hop acids, polysaccharides, polyphenols, lipids and divalent metal cations. Among these the interactions of hop acids, proteins and divalent metal cations promote the foam stability with minor help of polysaccharides and polyphenols (Evans and Bamforth, 2008; Steiner et al., 2011).

2.1.1 Beer proteins

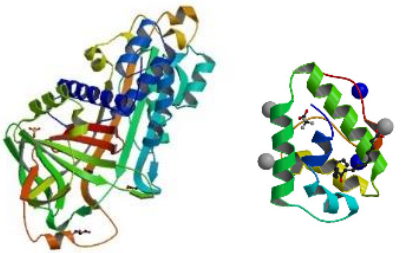

Figure 1. The structure of Serpin-Z4 (left) and LTP1 (right) from barley. Each colour of protein structure denotes properties of strand such as blue; Hydrophobic amino acid, red; Positively charged amino acids, green; Polar amino acids (Haas et al., 2013; Lampl et al., 2010; Lascombe et al., 2009).

Proteins are classified as albumins (water-soluble), globulins (salt-soluble), prolamins (alcohol-soluble) and glutelins (alkali-soluble). Here, only albumins involving α-amylase, protein Z and lipid transfer proteins (LTP) and prolamins which is called hordeins in barley are considered since they influence foam formation and stabilization (Steiner et al., 2011). The structure of proteins can be seen in Figure 1. However, the structure of proteins does not reflect modification during beer processing and Z4-serpin structure has identified only 49% (Haas et al., 2013).

Beer contains about 500 mg/L of proteinaceous components including various polypeptides with molecular weight ranging from less than 5 to over 100 kDa (Steiner et al., 2011). These polypeptides are emanating from barley, barley malt, and yeast in beer, however, yeast proteins are only minor constituents. Proteins are

modified by glycation, acylation and structural unfolding and become surface-active during beer brewing process such as mashing, wort boiling, fermentation and maturation. Only one-third of the total protein content left after these processes. Among them, all proteins related to foam formation were found to be glycosylated in different level. The size of the polypeptides forming glycoproteins was from 10 to 46kDa. These proteins in beer can be divided into three major groups; proline-rich polypeptides from hordein (15 to 32 kDa), LTP1 (9.7 kDa in pure form) and protein Z (40 kDa) (Steiner et al., 2011).

There are two contrasting theories concerning the foaming properties of polypeptides in beer. The first side is called *the discrete protein hypothesis*, and it claims that certain proteins, protein Z and LTP1, influence foam stability. The other side, which is termed as *the generalised amphipathic polypeptide hypothesis,* claims that diverse polypeptides (including protein Z and LTP) stabilize foam and the more hydrophobic their characteristics, the more foam promoting they are. For example, hordeins that are abundant in proline, glutamine and a hydrophobic β-turn. However, the foam from both albumins and hordeins are even more stabilized by hop acids (Bamforth and Kanauchi, 2003; Steiner et al., 2011).

2.1.2 Hop acids

Hops are prominent ingredients for brewing beer even though only a fraction of the significant amount of malt used is needed. The most important attribute of hops is the bitter taste and another feature is beer foam-stabilising effect. These are due to the hydrophobicity of isohumulones originating from hops. Isohumulones are converted from humulones by isomerisation during the wort boiling and it can be seen in Figure 2 (De Keukeleire, 2000).

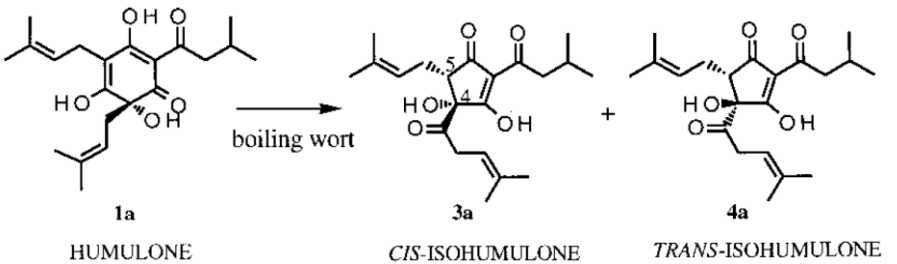

Figure 2. Structural change of humulones to isohumulones during the wort boiling (De Keukeleire, 2000).

The chemical structure of isohumulone shows hydrophobic characteristics due to the three side chains. This plays an important role in beer foam stability via hydrophobic interactions with amphiphilic polypeptides (Hughes, 2000). Isohumulones are deprotonated and become anionic in beer due to its low pKa (~3.1) compared to the pH (~4) of beer (Bamforth and Kanauchi, 2003). The anionic charge due to the deprotonation is delocalized over a cyclic β, β-triketone moiety and this enables to chelate metal cations producing an uncharged complex Especially, hop acids are able to form complexes with Cu^{2+} and Fe^{2+} ions (Hughes, 2000; Wietstock et al., 2016). The structure of hop acid-Fe^{3+} complexes is presented in Figure 3.

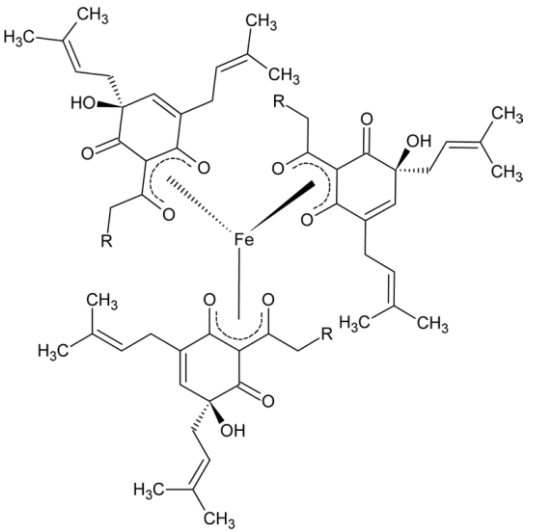

Figure 3. Schematic structure of humulone-Fe^{3+} complexes at pH 4.3 (humulone : Fe^{3+}, 3:1) (Wietstock et al., 2016)

A study revealed that pre-adsorbed hop acids at the vacuum-water interfaces reduce the free energy of protein adsorption and elevate it. Moreover, hop acid can self-associate themselves and then bind to the surface of LTP by hydrophobic interaction and this acts as a bridge exerting cross-linking of adsorbed proteins (Euston et al., 2008). The conformational structure of hop acid aggregates and protein-hop acid complex can be seen in Figure 4.

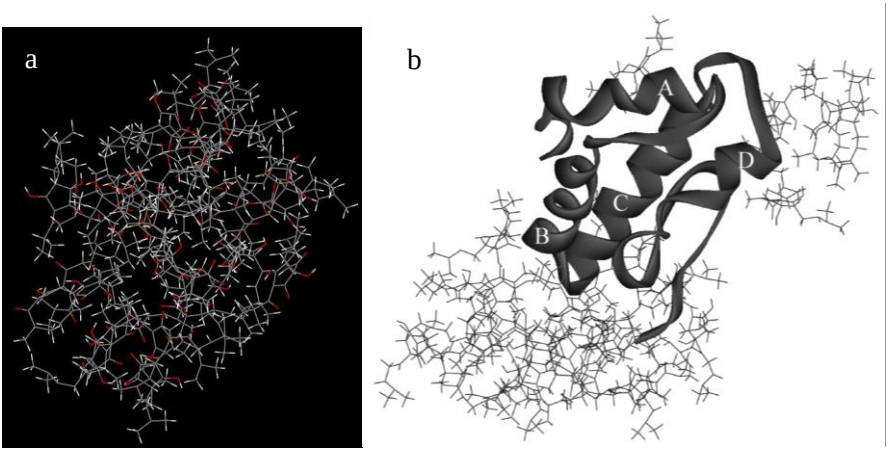

Figure 4. (a) Conformation of 24 cis-isocohumulone molecules in water system after 20 ns of molecular dynamics (MD) simulation at 300 K. The conformation apparently displays self-association of hop acid molecules in solution. (b) A complex of one LTP molecule with 24 cis-isocohumulone molecules simulated by PatchDock server. A-D represent each helix in LTP (Euston et al., 2008).

2.1.3 Hop acids-beer protein interactions

It has been suggested that hop acids can bind to the surface of LTP via hydrophobic interaction and possibly promote cross-linking of proteins in the adsorbed layer (Euston et al., 2008). The binding of hop onto the surface of LTP alters the tertiary structure of the protein, but not the secondary structure of it. It was also figured out that hop acids are greatly surface active and adsorb promptly to the vapor-water interfaces. In addition, the LTP seems to be highly attracted to the hop acid adsorbed layer and favourably adsorbs to such a layer compared to a clean vapor-water interfaces. As a result, hop acids promote beer foam stability by enhanced adsorption of LTPs at the interface (surface coverage by protein) and cross-linking of adsorbed LTPs with bridge formation between hydrophobic part on the LTP surface leading to increased mechanical strength in the adsorbed layer. This results in an enhanced interfacial viscosity and a decreased foam drainage rate (Euston et al., 2008).

2.2 Surface tension and Dilational modulus

Foams are dispersions of gas bubbles in liquid phase. In order to make foam, a certain amount of energy against the surface tension is required to counteract increase of the surface area (Bamforth, 1985).

The surface tension, γ is defined as (Dickinson, 1992):

$$\gamma = \left(\frac{\partial G}{\partial A}\right)_{p,T,n} \text{ [Eq. 1]}$$

where G is the Gibbs free energy, A is the surface area, p is the pressure, T is the temperature, and n is the overall amount of material in the system (Dickinson, 1992). The surface dilational modulus, E_d is determined by (Dickinson, 1992):

$$E_d = \frac{d\gamma}{d \ln A} \text{ [Eq. 2]}$$

The dilational modulus measures the change of surface tension compared to the surface area of adsorbed layer at the air-liquid interface. It shows the ability to resist compression and expansion of the layer (Aserin, 2008). The surface energy and tension are greatly reduced by surface active molecules modifying the properties of interface between air and liquid. Interactions between these molecules contribute to the surface rigidity of the foam (Bamforth, 1985). It was proposed that rigid proteins form more elastic adsorbed layers than flexible proteins do (Figure 5). This was because of its structural hardness within the protein network under compression and/or expansion (Cascão Pereira et al., 2003).

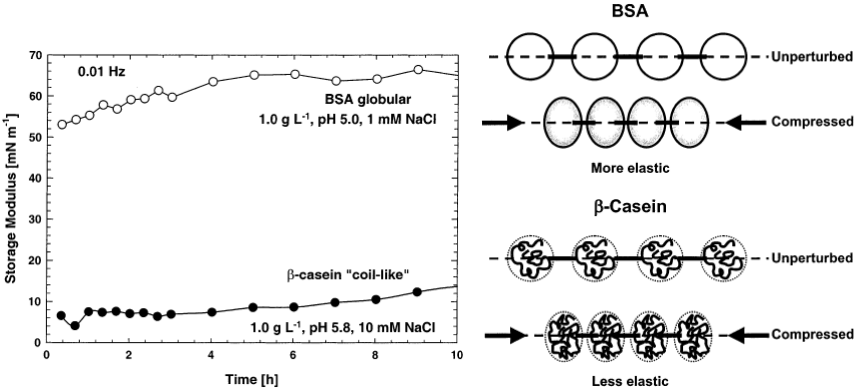

Figure 5. Dilational modulus of globular and rigid bovine serum albumin (BSA) and coil-like and flexible β-casein (left) and schematic of protein adsorbed layer under dilational deformation such as an interfacial area compression (Cascão Pereira et al., 2003).

2.3 Monolayer isotherm

Monolayer isotherm is a plot of surface pressure versus surface pressure the area per molecule of a surfactant. Upon compression, the states of the surfactant are changed. In gaseous state (G), the surfactants move independently but still they are anchored to the surface. In the liquid state, there are liquid expanded (LE) and condensed (C) states. The C state is more closely packed than LE state (Wigman, 2000). A typical monolayer isotherm can be seen in Figure 6.

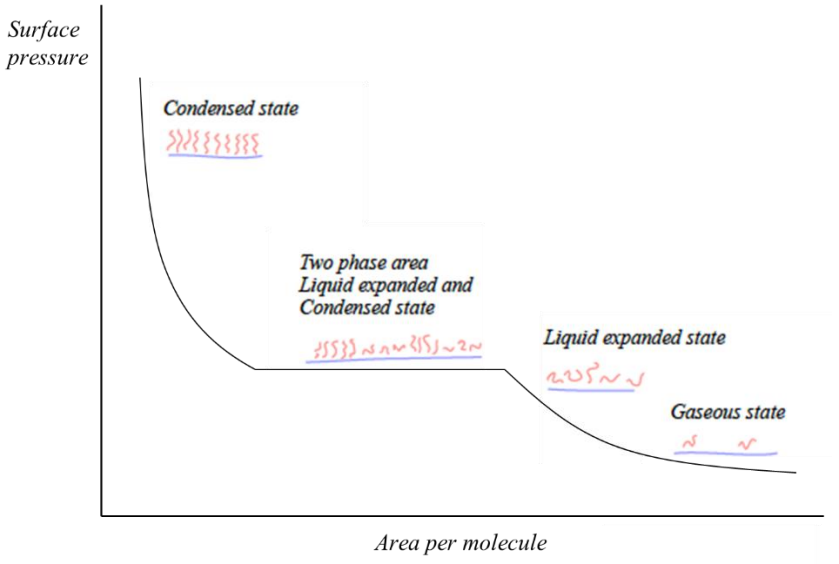

Figure 6. An illustration of the typical monolayer structures observed when a surface is compressed. (Modified from Hazell, 2014)

Typical structures of protein adsorbed layer are known as homogeneous at low surface pressure. Upon compression, it undergoes structural changes such as coiled state (loops) and further monolayer collapse (Figure 7). Certain proteins showed clear structural changes upon compression such as grouping in rows of circular domains for loops, stripes for phase transition from liquid expanded (LE) to liquid

condensed (C) and bright fringes or bright and dark islands for monolayer collapse (Bolaños-García et al., 2001; Toimil et al., 2012).

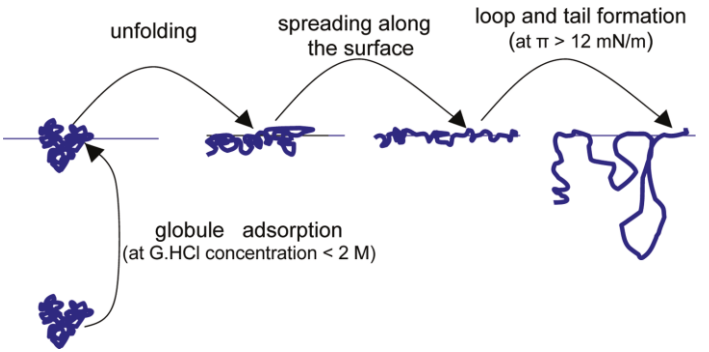

Figure 7. Scheme of the changes of BSA conformations during the process of adsorption (Noskov et al., 2010).

The adsorbed structures of surfactant domains exhibit various shapes at different condition. The stage from 0 to 1' in Figure 8 shows the formation of black domain and growth of it in area. At a certain point, the circular domains become unstable and change into symmetry-breaking shape such as an ellipse (2') and stripes (3'). The phase transition between stripes and hexagonal phase which is densely packed phase of circular domains (McConnell, 1991).

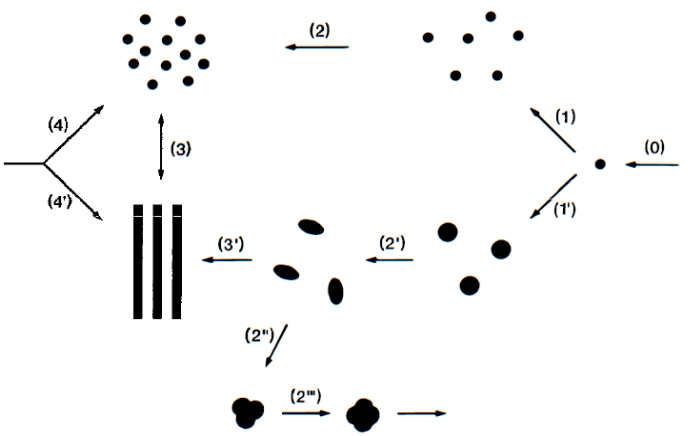

Figure 8. Theoretical explanation of surfactant domain structures and shape transitions that occur on the compression of a surfactant monolayer (McConnell, 1991).

3. Materials and Methods

3.1 Materials

3.1.1 Beer Proteins

Pale ale malt (Weyermann, Bamberg, Germany), was mashed in distilled water (4 kg/25 L) at 65℃ for 60 minutes and 75℃ for 10 minutes and it turned out pH 5.7 wort. This was boiled at 100℃ for 60 minutes and became boiled wort having pH 5.74. Protein content was measured by a nitrogen analyzer (Elemental Flash A 1112N, Thermo Fischer Scientific, Netherland). 100µL wort was burned in a sealed furnace at 950℃ and nitrogen content was quantified after GC separation and analysed by a thermal conductivity detector. The total protein percentage was determined by multiplying total nitrogen content with conversion factor of 6.25. Aspartic acid was utilized as the standard. Total carbohydrate was quantified using sulfuric acid and phenol digestion and measured by spectrophotometer under the wavelength of 490nm, as recommended by ASBC (beer-41). Total carbohydrate and protein content were confirmed as 0.1g/mL and 0.01g/mL respectively.

3.1.2 Isohumulone

Polaris pellet, 500 g (16.9% α acid, HHV, Mainburg, German) was boiled in 5 L of pH 4 acetate buffer (ionic strength 40 mmol/L), and it was centrifuged at 10.2k rpm (Allegra X-15R, Beckman Coulter Life Science, Indianapolis, Indiana) to eliminate precipitate. Supernatant, 100 mL was mixed with 2 mL of 85% H_3PO_4 in order to obtain pH 2 and 20 mL of isooctane was added to the supernatant. The mixture was kept in a rotary shaker overnight. After that the upper isooctane part was taken and removed. The solvent was evaporated under reduced pressure at room temperature. The glass was washed with acidified methanol (0.1 mL 85% H_3PO_4 in 100mL MeOH). The amount of iso-α acid was quantified by HPLC-DAD (Agilent Technologies 1260 Infinity, Santa Clara, US). ICS-I3 (total iso- 62.3 %, Labor Veritas, Zürich, Switzerland) was used as a standard. An isocratic elution was performed with 70% mobile phase A (MeOH), 30% B (0.1M EDTA solution with pH 2 modified by 85% H_3PO_4) at 0.5mL/min using a C18 reversed phase column (HALO C18, 4.6*150mm, 2.7µm, Berkshire, UK) at 275nm.

3.2 Methods

3.2.1 Measurement by Drop tensiometer

The surface tension and the dilational modulus were characterized using axisymmetrical drop shape analysis (ADSA) using a tracker from IT-concept, France.

The equipment needed to be calibrated before measurement. The calibration included things such as focus, uniformity of the illumination of the drop, verticality of the syringe needle and volumetric calibration. The calibration was confirmed by measurement of the surface tension of water. A surface tension of Milli-Q water was measured as 72±1 mN/m to ensure that the calibrations were properly conducted and reliability of further measurement. The setting for sinusoidal oscillation was amplitude 4mm^2, period 3 seconds with 6 active cycles and 8 blank cycles. The temperature of cuvette containing sample was kept at 25 ^{o}C using water bath. Each measurement started after discharging two drops of sample. All the measurements were performed in duplicated, and a new sample was injected into the syringe every time a new measurement was made, even for the same concentration, to avoid sedimentation of isohumulone. The surface tension and dilational modulus were calculated from active cycle (with large increment, 10000) in order to exclude noise from blank cycle. Detailed descriptions on measurement set-up are given below with Figure 9.

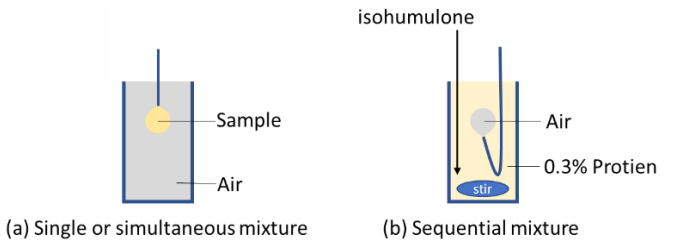

Figure 9. Schematic set-up for (a) single or simultaneous mixture and (b) sequential mixture

Single component and simultaneous mixture

An isohumulone sample (prepared from the Polaris hop), 4000 mg/L was diluted with pH 4 acetate buffer to 10, 25, 50, 75 and 100 mg/L. A protein sample (prepared from the pale ale malt), 0.6 % (w/w) was diluted to 0.1, 0.3 and 0.5%. For the simultaneous mixture, 0.3% proteins with varied isohumulone concentration was measured (Table 1). Every sample was mixed with a vortex for 30 seconds and the

density was measured. Straight needle was used for pendant method with 2.5 ml micro syringe. The syringe was attached to the equipment and the needle tip was placed inside cuvette to reduce the influence of the air flow. The initial droplet volume was 8 µl. It was measured/observed for 50 minutes. The last ten cycles were chosen for calculating surface tension and dilational modulus and the average was used for data analysis.

Table 1. Concentrations of pre-mixed protein and iso-alpha acid sample for simultaneous adsorption measurement with drop tensiometer

Protein (%)	Isohumulone (mg/L)
0.3	0
0.3	10
0.3	25
0.3	50
0.3	75
0.3	100

Sequential mixture

For the sequential mixture, cuvette was filled with 5 ml of 0.3% protein sample. The same but empty syringe connected to j-shaped needle was hanging to the equipment and immersed in protein solution. A bubble, 3.5 µl in volume was created and measurement had started from protein solution. After 10 minutes elapsed from measuring protein sample, 20 µl of Isohumulones (4000 mg/L) was added to the bottom of the cuvette using 100 µl micro syringe to prevent forming aggregate on top. The mixture of proteins and isohumulones was stirred and homogenized below the needle using magnetic stirring bar with moderate stirring speed. The addition of isohumulone was repeated every 10 minutes until the bulk concentration of isohumulone reached around 100 mg/L. The bulk concentration was calculated as Table 2. The first cycle and active cycle around every 100 seconds were calculated for surface tension and dilational modulus (data not shown). The last cycle for each concentration was used for data analysis.

Table 2. Protein and isohumulone concentrations of sequential mixture for drop tensiometer

Proteins (%)	Isohumulones (mg/L)
0.3	0
0.3	16
0.3	32
0.3	47
0.3	63

0.3	78
0.3	94

3.2.2 Observation by BAM

Procedure before observation

A calibration scale was utilized for focusing check. A filter paper was placed on a stand and height was adjusted to find the right image. A knob for focusing was changed to be focused on middle point of image with calibration scale. The polarizer and analyzer were adjusted by manually and "Measure in ROI" function, which optimizes the setting of polarizer and analyzer towards minimum light intensity was performed (Figure 10).

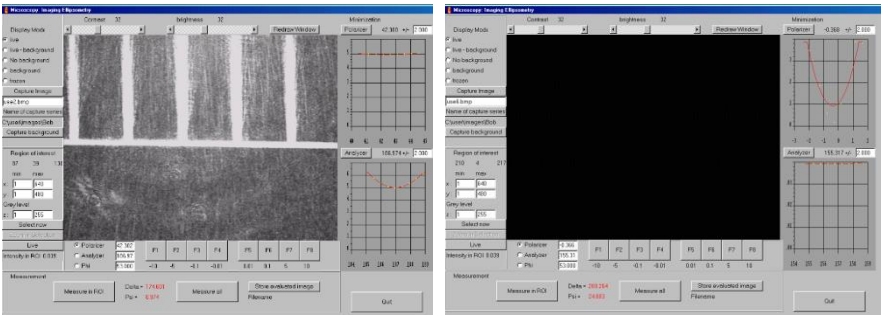

(a) (b)

Figure 10. An image of software programme "Multi" for Brewster angle microscopy. The alignment of polarizer and analyzer needed to be optimized for every sample. The incident angle (Phi) of laser is always set as 53º. Two graphs on the right in the programme show intensity of light versus the angles for polarizer and analyzer. (a) The setting was optimized for middle focusing with calibration scale (b)The setting was optimized for MiliQ water and it gave totally black image.

A glass pillar, black glass and petri dish were immersed in diluted Hellmanex (a strong alkaline detergent provided by Hellma Analytics, Müllheim, Germany) and washed out thoroughly with MiliQ water more than 15 times. They were placed on a stand as Figure 11-a. 40 ml of MiliQ water was poured onto the petri dish to ensure that the water level was more than 3 mm. To keep the same liquid level, that point was marked. The height of stand was adjusted to find the right condition for Brewster angle at air-water interfaces. A clean pipette attached to the water jet vacuum pump was used to remove impurities on the surface. The cleaning procedure was repeated until the surface had almost nothing (Figure 11-b).

(a) 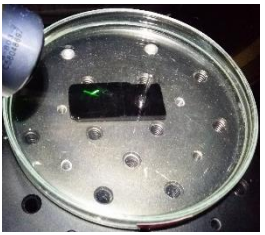 (b) 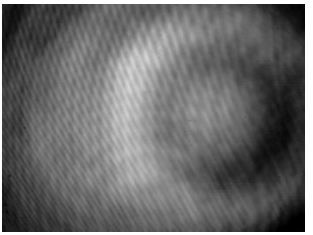

Figure 11. (a) Apparatus for Brewster angle microscopy. A glass pillar helped to add sample gently to the surface. A black glass with slope was used to inhibit reflection from the glass material. (b) Cleaned surface of MiliQ water without optimization of light setting. This interference ring shape can be seen in all the images. This was not able to control, and it should be considered as optical phenomenon, not as difference in thickness.

Observation of adsorbed layer

Isohumulone adsorbed layer

Isohumulone, 1000 mg/L was subjected under observation with no further addition of other sample.

Sequential adsorption layer

0.3% protein solution was used as subphase it was poured onto the petri-dish using measuring cylinder and observation continued for 10 minutes. Isohumulone sample, 1000 mg/L was added gradually from 50 to 300 µl. The concentration was calculated as Table 3.

Table 3. Summary of sequential adsorption layer and calculated concentration.

Subphase 0.3% protein	Concentration (mg/L)	volume (ul)	Surface concentration (mg/m2)[1]	Bulk concentration (mg/L)[2]
Sample Isohumulone	1000	50	7	1
		100	14	2
		150	21	4
		200	28	5
		250	35	6
		300	41	7

1. Assuming that all material is distributed at the surface of the petri-dish.
2. Assuming that all material is distributed in the bulk of the liquid in the petri-dish

Simultaneous adsorption layer

pH 4 acetate buffer was used as subphase and protein/isohumulone mixture was added to the surface from 200 to 1000ul. The concentration was calculated as Table 4.

Table 4. Summary of simultaneous adsorption layer and concentration calculation.

Subphase pH 4 buffer	Concentration	volume (ul)	Protein concentration		Isohumulone concentration	
			Surface[3] (mg/m2)	Bulk[4] (%)	Surface[3] (mg/m2)	Bulk[4] (mg/L)
Mixture of protein and isohumulone	Protein (%)	200	58	0.001	16	3
	0.21	400	116	0.002	32	6
	Isohumulone (mg/L)	600	174	0.003	47	8
		800	232	0.004	63	11
	571	1000	290	0.005	79	14

3. Assuming that all material is distributed at the surface of the petri-dish.
4. Assuming that all material is distributed in the bulk of the liquid in the petri-dish

4. Results and Discussion

4.1 Surface tension and dilational modulus

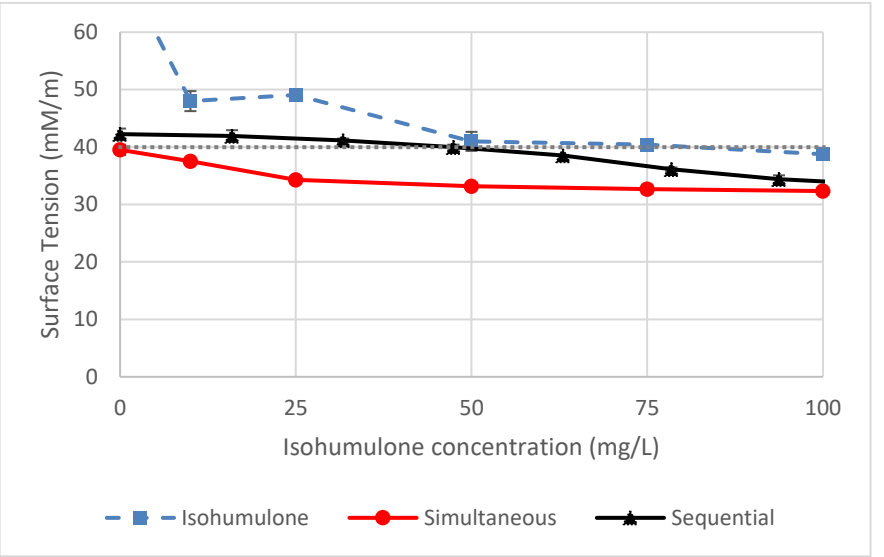

Figure 12. Surface tension of isohumulone in buffer solution (blue square), mixed sample of 0.3% protein and isohumulone in a simultaneous (red circle) and sequential way (black triangle). The lines between data were given as guideline for eyes. The gray dotted line was the surface tension of 0.3% protein and it was displayed for comparison. The measurement was duplicated, and the standard deviation of the data is presented with error bars.

The surface tension of each sample as a function of isohumulone and addition order is shown in Figure 12. The isohumulone shows surface activity and reduces the surface tension to about 40 mN/m at 50 mg/L. Also, the heat resistant water-soluble barley proteins [HRSBP] display surface activity and decrease the surface tension to 40 mN/m at 0.3 % protein. The surface tension in the presence of both isohumulones and proteins depends on the way of addition.

Sequential addition of isohumulone to a protein solution with a stabilized air-water interfaces exhibits a synergistic reduction of the surface tension above 50 mg/L of isohumulone concentration. However, the mixture of isohumulones and proteins allowed to equilibrate before the interface is formed shows a synergistic reduction of the surface tension at 10 mg/L of isohumulone concentration.

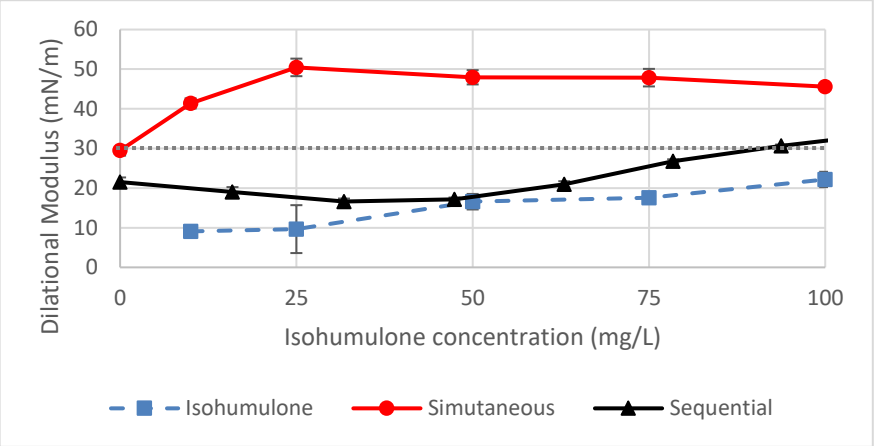

Figure 13. Dilational modulus of isohumulone (blue square), mixed sample of 0.3% protein and isohumulone in a simultaneous (red circle) and sequential way (black triangle). The lines between data were given as guideline for eyes. The gray dotted line was the dilational modulus of 0.3% protein and it was displayed for comparison. The measurement was duplicated, and the standard deviation of the data is presented with error bars. Simultaneous and sequential mixture had different moduli at 0 mg/L isohumulone which means containing only protein sample. This was because the time duration for the experiment was not the same (Simultaneous; 50 minutes and Sequential; 10 minutes). It was hard to prolong measurement time for sequential adsorption since a bubble hanging to the needle was easy to be released. However, overall trend of results did not change even though the measurement time of all the data was changed into 10 minutes. Hence, isohumulone containing samples were not influence above 25mg/L and protein line would be decreased to 25 mN/m. Thus, the data were not modified regarding measurement time.

The dilational modulus of each sample as a function of isohumulone and addition order is shown in Figure 13.The dilational modulus of isohumulone in the buffer solution increased continuously and reached 20mN/m at concentration 100mg/L. 0.3% protein reached 30mN/m which was even higher than that of isohumulone at quite high concentration. For sequentially added samples, the modulus decreased by little to 17mN/m by the addition of isohumulone and increased up to 30mN/m with more isohumulones. However, the modulus of pre-mixed sample went up to 50mN/m with rather small amount of isohumulone. It was noticeable that there was huge gap in modulus between simultaneously and sequentially prepared samples.

Pre-mixed sample was more effective in lowering surface tension compared to sequentially added sample and the modulus of pre-mixed one was exceptionally high compared to any other samples. Thus, a possible explanation for simultaneous sample was that beer protein-isohumulone complex was formed when they were mixed, and it is more surface active and changes into more rigid structure. It was suggested that interfacial dilational modulus is more affected by the adsorbed molecular structure than the adsorbed amount (Cascão Pereira et al., 2003). Indeed, there was a conformational change of LTP induced by formation of protein-hop acids complex although it was limited to a small change considering a significant amount of hop acids (24 molecules for a protein) bound to it (Euston et al., 2008). There is another contribution to the high modulus of adsorbed proteins that is interprotein network arising from their conformational rearrangement or unfolding at the air-water interface (Cascão Pereira et al., 2003). However, this does not play an important role in beer sample. The reason is that the protein-hop acids complex showed little conformational change at air-water interface as mentioned earlier. Instead, isohumulones enhance the rigidity of the protein network by cross-linking or cementing proteins in the adsorbed layers (Bamforth and Kanauchi, 2003; Euston et al., 2008).

The tension and modulus of sequential mixture differed from those of simultaneous one, but they were somewhat correlated with data from isohumulone. The surface tension of isohumulone was decreased greatly at the concentration of 50mg/L and it was not changed by further addition of isohumulones up to 250 mg/L (data not shown). Above that concentration, the surface tension was retained which means the surface was fully saturated with isohumulones. For the modulus of isohumulone, it also increased drastically at 50mg/L and kept increasing gradually up to 28 mN/m at 250 mg/L (data not shown). Therefore, it was concluded that the isohumulones formed multilayer above a certain point as they were kept accumulating at the air-water interface providing continuous increase of dilational modulus. This result was in agreement with the continuous adsorption of isohumulones at hydrophobized solid-aqueous interfaces confirmed by ellipsometry performed by Yi Lu.

The surface tension and dilational modulus of sequential mixture slightly changed when there was not enough isohumulone (below 60 mg/L) and they were similar to the value of protein adsorbed layer from the beginning (0 mg/L). Above 60 mg/L of isohumulones, both properties demonstrated greater changes and were enhanced in terms of foam-positive effect compared to those of individual components. Consequently, it seemed that the sequentially adsorbed layers were dominated by proteins at first and by protein-isohumulone complex at the end.

Shallow minima of dilational modulus between 30 to 50 mg/L can be interpreted as disturbance of adsorbed protein layers caused by adding isohumulones. This behaviour can be explained as orogenic displacement which shows displacement of adsorbed protein layer at the air-water interface by increasing surfactant concentration (Morris and Groves, 2013). This interpretation is probable but there is no direct data showing any structural change of the adsorbed layers. Thus, these data need to be combined with BAM images of adsorbed layers at the air-water interfaces.

4.2 BAM image

All the BAM images were qualitatively analysed by comparing with BAM images from other literatures. This is because no other complementary equipment such as Langmuir trough was used to obtain monolayer isotherm. However, it was claimed that experiments conducted with the density change of surfactant by consecutive addition at interfaces were more reproducible and reliable than using mechanical apparatus allowing compression and expansion of adsorbed film (Moore et al., 1986). The mobility of domains on the adsorbed layer was calculated based on the processed images over a short period of time using a function (image calculator) from a software, Image J. A certain condition from each system was chosen which had domains that can be tracked. The mobility of different system is presented in Figure 17.

4.3.1 Isohumulone adsorbed layer

There were variety of adsorbed structures with the addition of isohumulone by spreading over the air-water interfaces of the buffer surface. Isohumulone was readily adsorbed at the interfaces and showed these structures immediately. All these structures were distributed over the whole surface and existed at the same time. The surface appeared fluid-like and observed objects were moving over the surface. The structures of isohumulone adsorbed layers are shown in Figure 14. The adsorbed layer was highly heterogeneous.

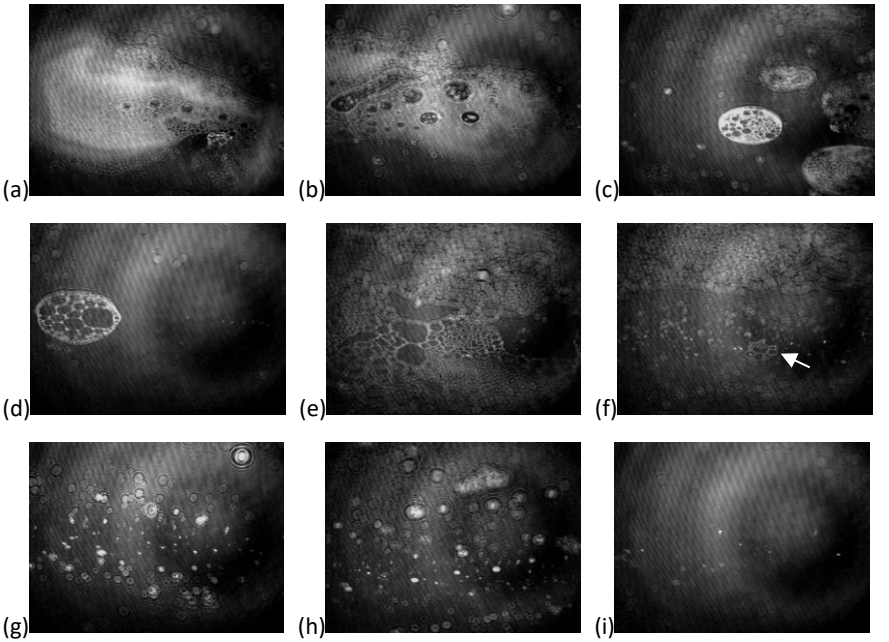

Figure 14. BAM image of Isohumulone adsorption layer. (a) Large bright domains with dark holes, (b) Large bright domains with dark holes and dispersed bright circular domains, (c) Small circular domains with dark holes, (d) 2D foam-like circular domain, (e) Large 2D foam-like domain, (f) Highly condensed small circular domains with small 2D foam-like domain (white arrow), (g and h) Highly bright circular and irregular domains and (i) regions with less domains. All images are 100 µm×75 µm. The images provided are chosen from over 1000 taken of the same surface and are intended to represent what was observed. The images were compared with other BAM images and they are presented in Appendices 1 to 6.

4.3.2 Sequential adsorption layer

0.3% protein solution was allowed to adsorb at the interfaces and 1000 mg/L of isohumulone was gradually spread over the surface and remained for adsorption as well (1 to 7 mg/L calculated as bulk concentration). The BAM images of sequential addition of isohumulones onto protein adsorbed layer are presented in Figure 15. The adsorbed layer appeared firm as it was hardly moving at all and mostly the same stripes were seen out of entire surface of petri dish (Figure 15-f to l). Therefore, when the bulk concentration of isohumulone reached 7 mg/L, the structure of adsorbed layer was checked at different observation point by moving petri dish very gently and other structures can be seen (Figure 15-m to s).

Composition		
0.3 % protein subphase	+ 2 mg/L isohumulone	
(a) 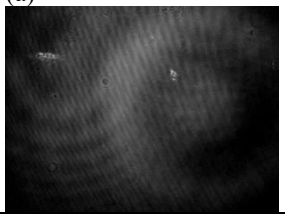	(b) 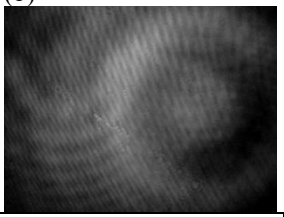	(c) 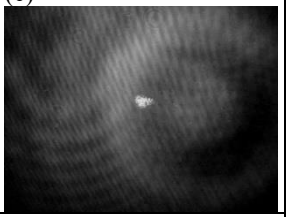
+ 4 mg/L isohumulone		+ 5 mg/L isohumulone
(d) 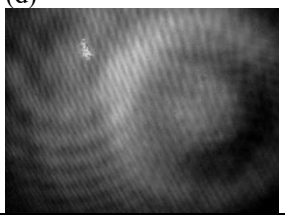	(e) 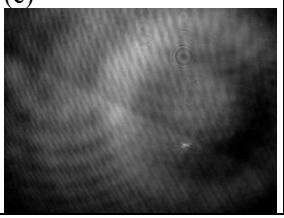	(f) 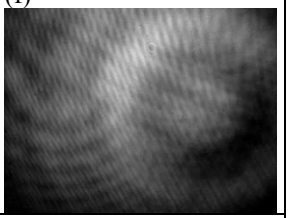
+ 6 mg/L isohumulone		
(g) 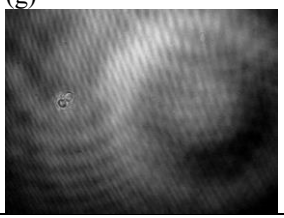	(h) 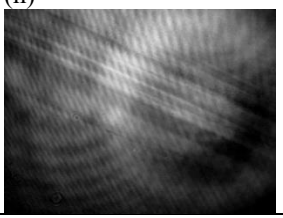	(i) 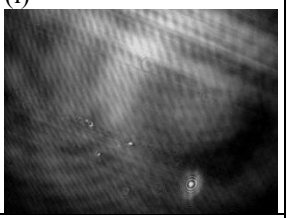
+ 7 mg/L isohumulone		
(j) 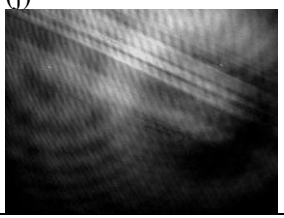	(k) 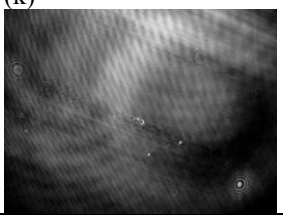	(l) 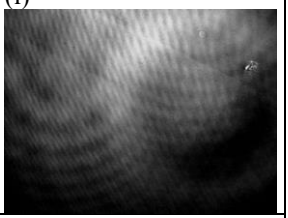
(m) 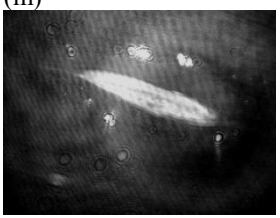	(o) 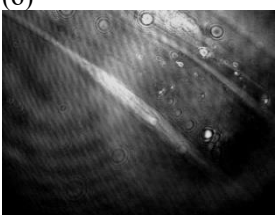	(p) 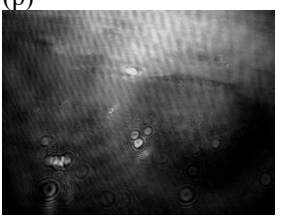

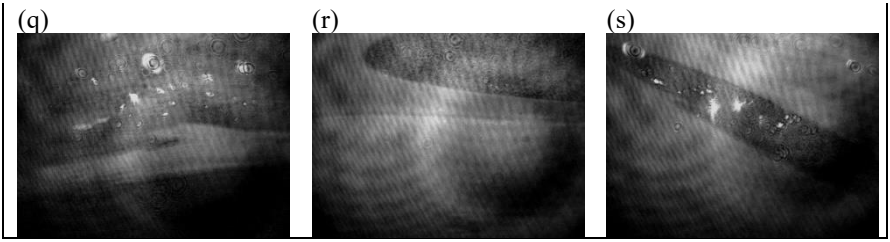

Figure 15. BAM images of sequential adsorption layer. (a) dark circular domains and bright irregular domains, (b) grouping of circular domains in rows, (c and d) bright irregular domains, (e) bands with different brightness, (f to l) stripes with or without bright circular domains, (m and o) large bright island with bright circular and irregular domains, (p and q) mixed regions with different brightness and bright circular domains and (r and s) large dark domains with or without bright circular domains. All images are 100 µm×75 µm. The images provided are chosen from over 300 taken of the same surface and are intended to represent what was observed. The images were compared with other BAM images and they were presented in Appendices 7 to 13.

4.3.3 Simultaneous adsorption layer

0.6 % Proteins and 1000 mg/L isohumulone solution were mixed and allowed to equilibrate. This mixture was spread over the surface of the buffer subphase. The structure of simultaneous adsorption layer of proteins and isohumulones are presented in Figure 16. As more sample was added, the more circular domains were observed.

Composition		
0.001 % proteins + 3 mg/L isohumulones	0.002 % proteins + 6 mg/L isohumulones	
(a)	(c)	(d)
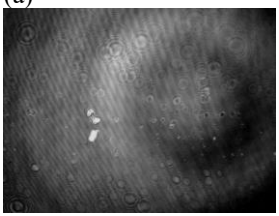	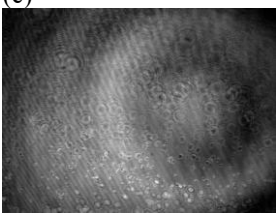	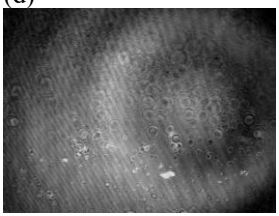

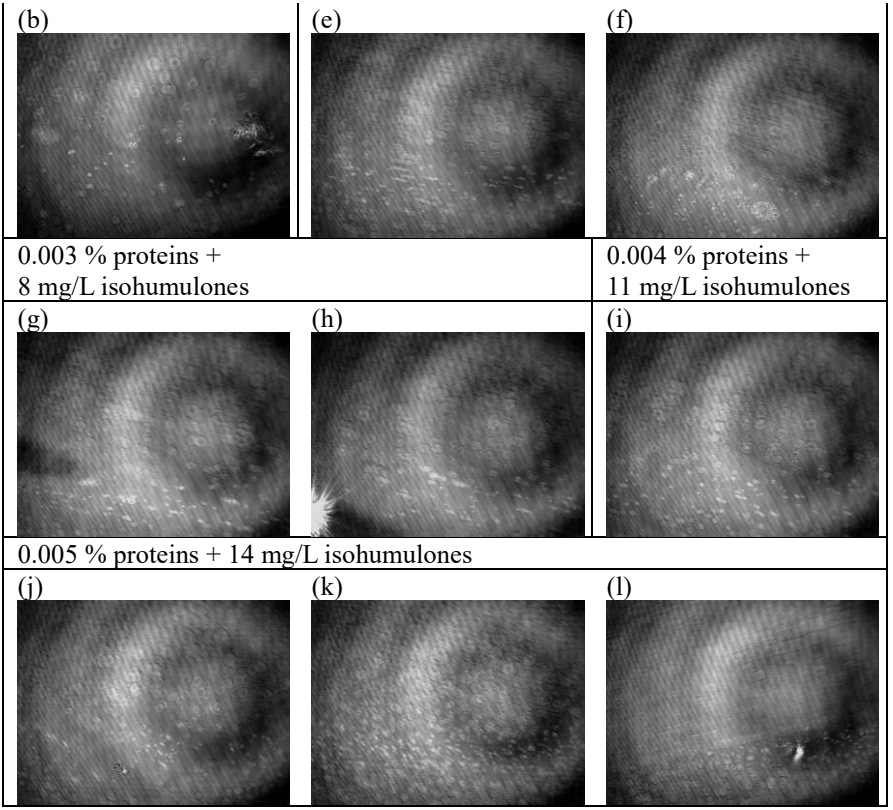

Figure 16. BAM image of simultaneous adsorption layer. All the images possessed circular domains. (a) circular and bright irregular domains, (b) cluster of circular domains, (c and d) densely packed circular domains and bright irregular domains, (e) grouping of circular domains in rows, (f) large cluster of circular domains and frontier between two different regions, (g and h) dark regions with or without bright spot, (i) bright region, (j) grey region, (k) highly condensed circular domains and (l) frontier between two different regions and bright circular domain. All images are 100 μm×75 μm. The images provided are chosen from over 500 taken of the same surface and are intended to represent what was observed.

The adsorbed layer of each system was clearly distinct from each other.

The layers appeared semi-fluid. Hence, a tentative evaluation of the mobility of domains was made and it can be seen in Figure 17. From the results, it is clear that the obtained fluidity varies significantly over time. The mobility of domains of all the system was rather similar at the beginning after 1 minute had passed. Domains of the isohumulone adsorbed layer continued to move fast regardless of

time. However, the mobility of domains drastically slowed down by factor of 10 in sequential adsorption after 16 minutes compared to that of 1 minute. The mobility of domains decreased after 20 minutes passed in simultaneous adsorption. Thus, the isohumulone adsorbed layer was highly movable independent of time passed. Adsorbed layer of sequential mixture was extremely firm after 16 minutes had passed and hardly moved. The adsorbed layer formed in a simultaneous way became stabilized after 20 minutes passed and the mobility decreased slightly.

Time (min)	Image 1	Image 2	Processed image	Rate (μm/s)
	Isohumulone 1000 mg/L			
t=1		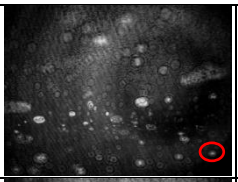	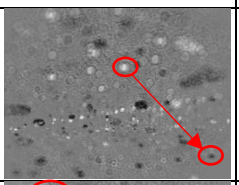	4.0
t=20	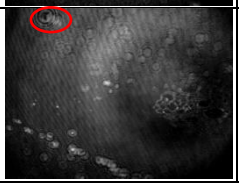		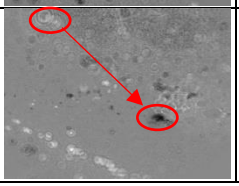	6.9
	Sequential 0.3 % protein + 7 mg/L isohumulone			
t=1	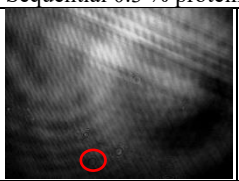	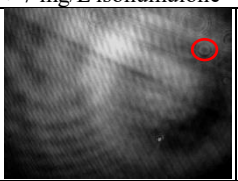	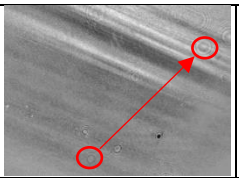	4.5
t=16	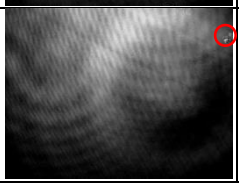	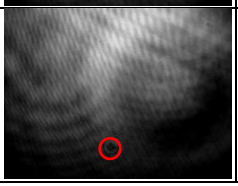	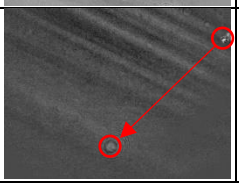	0.4
	Simultaneous 0.001 % protein + 3 mg/L isohumulone			
t=1	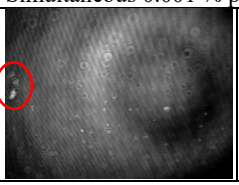	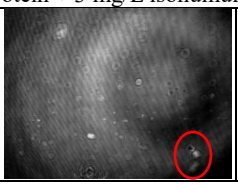	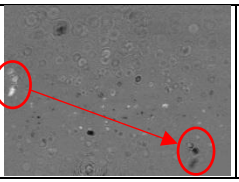	5.5

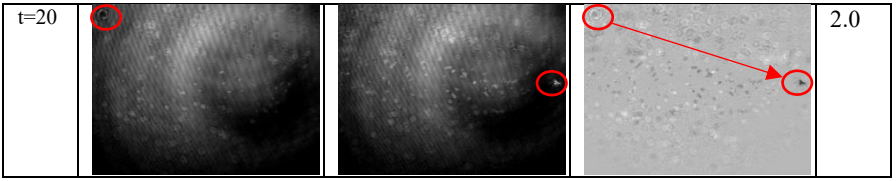

Figure 17. BAM image analysis regarding the rate of domains at different conditions such as isohumulone, sequential and simultaneous mixture. A specific domain was chosen and tracked to calculate the rate of it at the interface. All images are 100 µm×75 µm.

Figure 14-a obtained from pure isohumulone shows large liquid condensed (C) domains (bright domains) with dispersed gas (G) or liquid expanded (LE) phases (dark holes). In Figure 14-b, it shows similar structure to Figure 14-a but it holds much larger dispersed G or LE phases containing small C domains. Figure 14-c and d display increased number of dispersed G or LE phases in circular C domains. These dispersed G or LE phases in Figure 14-d seem much bigger and the areas or lines between the holes (C phase) are smaller or thinner. This presents 2D foam-like structure [Appendix 1 to 5]. The foam-like structure is spread over a large area and the shape of dispersed G or LE phases is irregular rather than circular. In Figure 14-f, it demonstrates highly condensed small circular C domains with small foam-like domain. This is regarded as under the phase transition from the C to the LE phase. In this situation, the network structure "melted away" within a few minutes (Hönig, Overbeck and Mobius, 1992). Figure 14-g and h exhibit aggregates of isohumulones because they give much brighter and larger domains compared to C domains. Hop acids are able to associate themselves and form aggregates (Figure 4-a). Hence, the BAM image of these structures are very similar to that of a non-conventional surfactant, which is macrocyclic surfactant, para-tert-butylcalix[6]arene (Calix6) (de Lara et al, 2016). It was suggested that Calix6 aggregates as dimer at the air-water interfaces [Appendix 6]. Figure 14-i shows G or LE phase with some C domains and aggregates. These images can be further divided into a network consisted of C domain and G or LE phases (Figure 14-a to f), isohumulone aggregates (Figure 14-g and h) and G or LE phases with C domains and aggregates (Figure 14-i). 2D foam structure is ubiquitous in monolayer either as G/LE coexistence or reverse LE/LC phase transition. The images (Figure 14-a to f) seem to be the latter one because the bulk concentration of isohumulone is fairly high, 1000 mg/L. Consequently, the morphology of isohumulone adsorbed layer is highly heterogeneous and this may be because of its tendency to self-association causing formation of isohumulone aggregates.

The adsorbed layer of beer proteins showed circular domains when there was no or little isohumulone (Figure 15-a) [Appendix 7 to 9]. When more isohumulones were added, grouping of circular domains can be seen which implies structural changes or rearrange of adsorbed proteins (Figure 15-b) [Appendix 9]. More pronounced changes can be seen such as bands with different brightness and stripes with some bright aggregates, indicating coexistence of phases or phase transition (Figure 15-e to l) [Appendix 7, 9, 10 and 11]. Other structures were observed at different observation point such as collapsed protein island (Figure 15-m and o) [Appendix 7, 8, 10 and 12], bright protein-rich region and dark isohumulone-rich region with its aggregates (Figure 15-p and q) [Appendix 10 and 11] and highly condensed isohumulone C domains with its aggregates (Figure 15-r and s) [Appendix 11]. Overall, these structures can be divided into protein-dominant regions (Figure 15-a to l), mixed regions of protein-rich including collapsed protein island and isohumulone-rich including isohumulone aggregates and C domains of isohumulones (Figure 15-m to s). Thus, the adsorbed layer formed in a sequential way displayed separate regions rich in either isohumulone or proteins.

The adsorbed layer of simultaneous mixture displayed circular domains in all the images. At low concentration, circular domains were distributed sparsely over the surface (Figure 16-a and b). As the concentration of the sample increased, the number of circular domains increased and the domain shape changed from sparsely distributed circular domains to hexagonal lattice phase. As the size of domain increases, it becomes unstable and is subjected to the transition to an ellipse and further to the stripes. The hexagonal and stripes phases are able to coexist (McConnell, 1991). Thus, simultaneous adsorption forms an adsorbed layer mainly consists of two different phases, which are dispersed circular domains and a continuous phase.

5. Discussion

The surface rheology by the tensiometric experiments shows that both the beer protein fractions and the isohumulone fractions are surface active. The mixture of isohumulones and beer proteins exhibit synergistic effects on interfacial rheology. However, rheological properties were influence by the sequence of addition and the concentration of isohumulones.
BAM images of isohumulones and mixtures display clearly different structures from each other. The adsorbed layer with isohumulones is fluid-like and with mixture is rather solid-like. The sequentially adsorbed layer has less mobility over time compared to the simultaneously adsorbed one. It seems contradictory to the results from tensiometry. However, the obtained mobility does not represent the properties of a certain system and the concentration should be also considered. This is because the condition of mobility in sequential adsorption is in the range of protein-rich region, containing 0.3 % proteins and in simultaneous adsorption, it has further lower concentration of proteins and higher amount of isohumulones, 0.001 % and 3 mg/L.

The different dilational modulus of the different surface layers can partly be understood from the Takayanagi theory of mechanical properties of dispersions, Figure 18 (Quiroga and Bergenståhl, 2008).

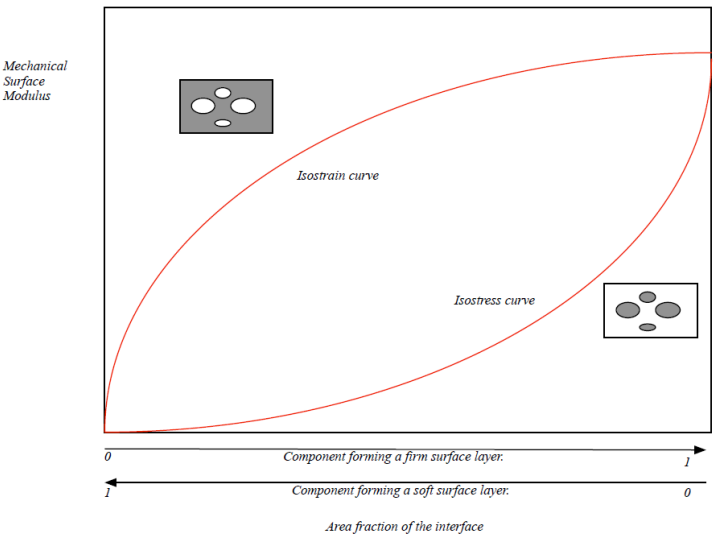

Figure 18. Takayanagi theory of mechanical properties of dispersions. Depending on if the continuous phase is firm or soft, the properties of the dispersion will follow different curves. If the continuous material is the firm component of the dispersion the mechanical properties will follow the isostrain curve (both the soft and the firm objects are deformed equally). If the continuous material is the soft component of the dispersion the mechanical properties will follow the isostress curve (both the soft and the firm objects are exposed to equal stress).

A single component surface layer is expected to pass through a sequence of phase transitions when the concentration at the surface is gradually increased. See Figure 6. Two components, isohumulones and beer proteins, were evenly distributed over the surface in simultaneous adsorption with a few isolations of proteins or isohumulones. The sequentially adsorbed layer displayed a variety of separated domains such as isohumulone-rich regions and protein-rich regions.

6. Conclusion

Both the soluble protein fraction in beer and the isohumulone display surface activity and contribute to the formation of the air water interfacial layer.

The properties of the surface film depends on the composition and of the addition sequence of the components. If added together as a pre-mixed solution the components form a firm surface layer. The surface layers display partial lateral phase separation. However, the continuous layer is firm, thus, most likely consisting of proteins or complexes of proteins and isohumulone.

If isohumulone is added to a protein surface, the dilatational data suggests that a partial depletion of protein can be obtained with reduced firmness. However, this effect may depend on time and concentrations.

7. References

Andersen, A. (2005). *Surfactants Dynamics at Interfaces A series of Second Harmonic Generation experiments*. Doctoral thesis. Universität Potsdam.

Aserin, A. (2008). *Multiple emulsions*. Hoboken, N.J.: Wiley-Interscience, pp.10-15.

Bamforth, C. (1985). The Foaming Properties of Beer. *Journal of the Institute of Brewing*, 91(6), pp.370-383.

Bamforth, C. and Kanauchi, M. (2003). Interactions between polypeptides derived from barley and other beer components in model foam systems. *Journal of the Science of Food and Agriculture*, 83(10), pp.1045-1050.

Bolaños-García V, Ramos S, Castillo R, Xicohtencatl-Cortes J, Mas-Oliva J. Monolayers of Apolipoproteins at the Air/Water Interface. *The Journal of Physical Chemistry B*. 2001;105(24):5757-5765.

Caro A, Nino M, Sanchez C, Gunning A, Mackie A, Patino J. Displacement of β-Casein from the Air–Water Interface by Phospholipids. In: Dickinson E, ed. by. *Food Colloids: Interactions, Microstructure and Processing.* 1st ed. Cambridge: The Royal Society of Chemistry; 2005. p. 160-175.

Cascão Pereira, L., Théodoly, O., Blanch, H. and Radke, C. (2003). Dilatational Rheology of BSA Conformers at the Air/Water Interface. *Langmuir*, 19(6), pp.2349-2356.

De Keukeleire, D. (2000). Fundamentals of beer and hop chemistry. *Química Nova*, 23(1), pp.108-112.

de Lara, L., Wrobel, E., Lazzarotto, M., de Lázaro, S., Camilo, A. and Wohnrath, K. (2016). An experimental and theoretical study of the aggregate structure of calix[6]arenes in Langmuir films at the water/air interface. *Physical Chemistry Chemical Physics*, 18(33), pp.22906-22913.

Dickinson, E. (1992). *An introduction to food colloids*. Oxford: Oxford University Press, pp. 30-78.

Euston, S., Hughes, P., Naser, M. and Westacott, R. (2008). Molecular Dynamics Simulation of the Cooperative Adsorption of Barley Lipid Transfer Protein andcis-Isocohumulone at the Vacuum−Water Interface. *Biomacromolecules*, 9(11), pp.3024-3032.

Evans, D., Surrel, A., Sheehy, M., Stewart, D. and Robinson, L. (2008). Comparison of Foam Quality and the Influence of Hop α-Acids and Proteins Using Five Foam Analysis Methods. *Journal of the American Society of Brewing Chemists*, 66(1), pp.1-10.

Evans, D.E., and Bamforth, C.W. (2008) Beer foam: achieving a suitable head. in *Handbook of alcoholic beverages: Beer, a quality perspective* edited by Bamforth, C.W., Russell, I., and Stewart, G.G., Elsevier Burlington MA, pp 1-60.

Gallier, S., Gragson, D., Jiménez-Flores, R. and Everett, D. (2010). Surface Characterization of Bovine Milk Phospholipid Monolayers by Langmuir Isotherms and Microscopic Techniques. *Journal of Agricultural and Food Chemistry*, 58(23), pp.12275-12285.

Gambut, L., Chauvet, J., Garcia, C., Berge, B., Renault, A., Rivière, S., Meunier, J. and Collet, A. (1996). Ellipsometry, Brewster Angle Microscopy, and Thermodynamic Studies of Monomolecular Films of Cryptophanes at the Air−Water Interface. *Langmuir*, 12(22), pp.5407-5412.

Haas, J., Roth, S., Arnold, K., Kiefer, F., Schmidt, T., Bordoli, L. and Schwede, T. (2013). *Protein Model Portal*. [online] Proteinmodelportal.org. Available at: https://www.proteinmodelportal.org/ [Accessed 23 Jan. 2018].

Hazell, G. (2014). *Surface Scattering from Soft Matter at Interfaces.* Doctoral thesis. University of Bath.

Heinig, P. (2003). *The geometry of interacting liquid domains in Langmuir monolayers*. Doctoral Thesis. Universität Potsdam.

Hönig, D., Overbeck, G. and Möbius, D. (1992). Morphology of pentadecanoic acid monolayers at the air/water interface studied by BAM. *Advanced Materials*, 4(6), pp.419-424.

Hughes, P. (2000). The Significance of Iso-α-Acids for Beer Quality Cambridge Prize Paper. *Journal of the Institute of Brewing*, 106(5), pp.271-276.

Lampl, N., Budai-Hadrian, O., Davydov, O., Joss, T., Harrop, S., Curmi, P., Roberts, T. and Fluhr, R. (2010). ArabidopsisAtSerpin1, Crystal Structure and in Vivo Interaction with Its Target Protease RESPONSIVE TO DESICCATION-21 (RD21*). Journal of Biological Chemistry*, 285(18), pp.13550-13560.

Lascombe, M., Prange, T., Bakan, B. and Marion, D. (2009). Three-dimensional structure of a post translational modified barley LTP1.

Markowitz, M., Bielski, R. and Regen, S. (1989). Ultrathin monolayers and vesicular membranes from calix[6]arenes. *Langmuir*, 5(1), pp.276-278.

McConnell H. Structures And Transitions In Lipid Monolayers At The Air-Water Interface. *Annual Review of Physical Chemistry*. 1991;42(1):171-195.

McConnell H. Structures and Transitions In Lipid Monolayers At The Air-Water Interface. *Annual Review of Physical Chemistry.* 1991;42(1):171-195.

Moore, B., Knobler, C., Broseta, D. and Rondelez, F. (1986). Studies of phase transitions in Langmuir monolayers by fluorescence microscopy. *Journal of the Chemical Society, Faraday Transactions 2*, 82(10), p.1753.

Morris, V. and Groves, K. (2013). *Food Microstructures*. Cambridge: Woodhead Publishing, pp.47-51.

Noskov, B., Mikhailovskaya, A., Lin, S., Loglio, G. and Miller, R. (2010). Bovine Serum Albumin Unfolding at the Air/Water Interface as Studied by Dilational Surface Rheology. *Langmuir*, 26(22), pp.17225-17231.

Quiroga, C. and Bergenståhl, B. (2008). Rheological behavior of amylopectin and β-lactoglobulin phase-segregated aqueous system. *Carbohydrate Polymers*, 74(3), pp.358-365.

Rodríguez Patino J, Niño M, Sánchez C, Fernández M. Whey Protein Isolate−Monoglyceride Mixed Monolayers at the Air−Water Interface. Structure, Morphology, and Interactions. *Langmuir*. 2001;17(24):7545-7553.

Rodríguez Patino, J., Rodríguez Niño, M. and Sánchez, C. (2003). Protein–emulsifier interactions at the air–water interface. *Current Opinion in Colloid & Interface Science*, 8(4-5), pp.387-395.

Steiner, E., Gastl, M. and Becker, T. (2011). Protein changes during malting and brewing with focus on haze and foam formation: a review. *European Food Research and Technology*, 232(2), pp.191-204.

Toimil P, Prieto G, Miñones J, Trillo J, Sarmiento F. Monolayer and Brewster angle microscopy study of human serum albumin—Dipalmitoyl phosphatidyl choline mixtures at the air–water interface. *Colloids and Surfaces B: Biointerfaces.* 2012;92:64-73.

Wietstock, P., Kunz, T., Pereira, F. and Methner, F. (2016). Metal Chelation Behavior of Hop Acids in Buffered Model Systems. *BrewingScience*, 69, p.56.

Wigman, A. (2000). *Applications of brewster angle microscopy to adsorbed species at the air/water interface.* Doctoral thesis. University of Durham.

8. Appendices

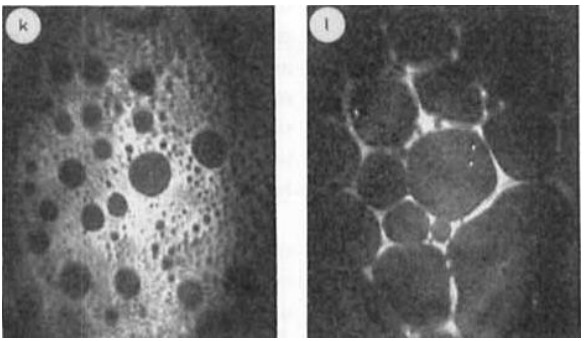

[Appendix 1] Pentadecanoic Acid monolayer visualized by BAM. Left: A network structure was formed with small holes and this seems to be comparable to the foam structure which can be observed in the gas/LE coexistence region Right: This network structure was observed below the surface pressure of phase transition from C state to LE, and it melted away in a few minutes (Hönig, Overbeck and Möbius, 1992)

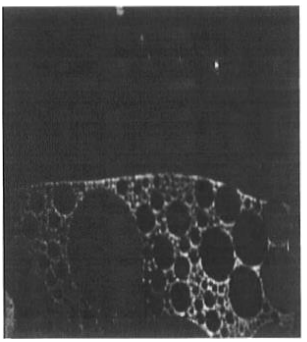

[Appendix 2] BAM image of a liquid-gas phase transition for a film of cryptophane 3. The dark domains correspond to water or to a gas phase, the gray areas seem to be a liquid phase. The 2D-foam formation was observed (Gambut et al., 1996).

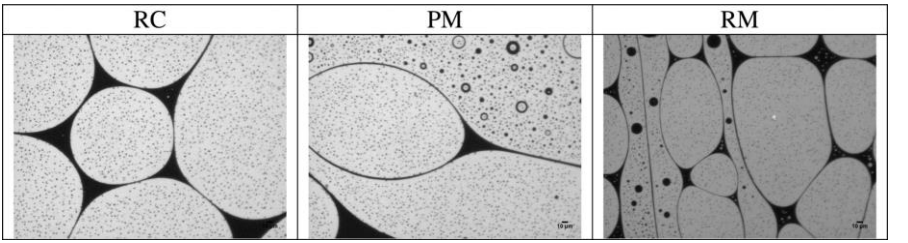

[Appendix 3] Epifluorescence microscope images of 2D-foam structure from prepared phospholipids monolayers extracted from bovine milk at different processing stage, raw cream (RC), processed milk (PM) and raw milk (RM). A gaseous phase is dark due to the low density of phospholipids regardless of labelling (Gallier et al., 2010).

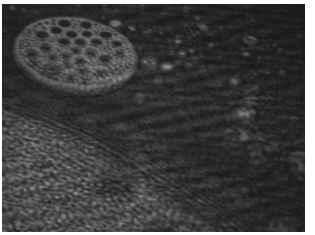

[Appendix 4] BAM image taken from a 2 mmol N-n-alkyl-4'-(dimethylamino)-stilbazium bromides (HC7) solution. The inhomogeneities in the form of 2D-foams at the air-water interface. This is because of the solubility limit in this solution. (Andersen, 2005).

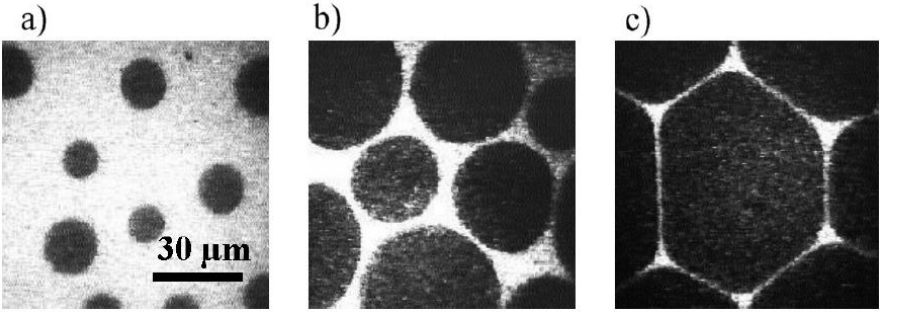

[Appendix 5] Images of a myristic acid monolayer obtained by fluorescence microscopy. Gaseous phase is immersed in a liquid expanded phase a) wet foams, b) and c) dry foams obtained by expansion (Heinig, 2003).

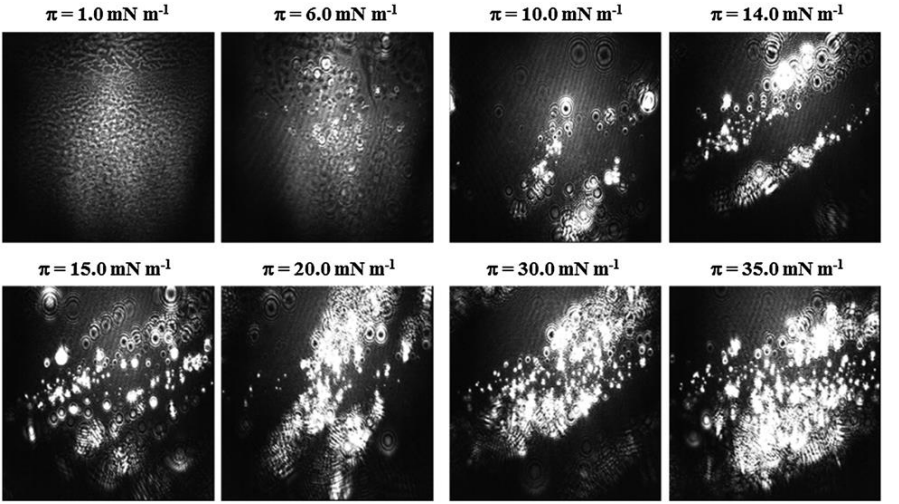

[Appendix 6] BAM images of para-tert-butylcalix[6]arene (Calix6) films at different surface pressures. Image size: 460 mm width (Markowitz, Bielski and Regen, 1989).

[Appendix 7] BAM images of apolipoproteins AII monolayer. Left: Just before LE/C transition, middle: LE/C coexistence and right: collapsed monolayer (Bolaños-García et al., 2001)

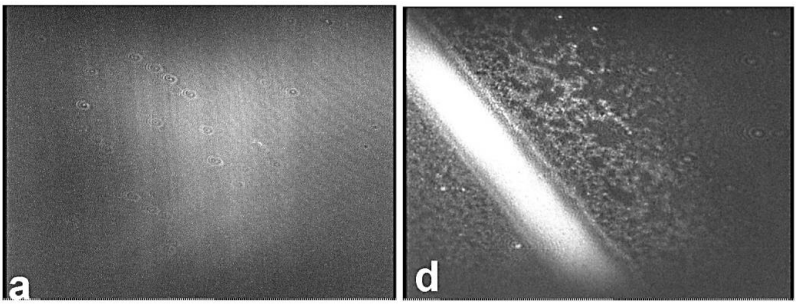

[Appendix 8] BAM images of pure protein (left) and protein and surfactant mixed film (right). Left: a homogeneous G or LE structure at all the surface pressure.

Right: the islands of collapsed protein in the mixed film at a high surface pressure (Rodríguez Patino, Rodríguez Niño and Sánchez, 2003).

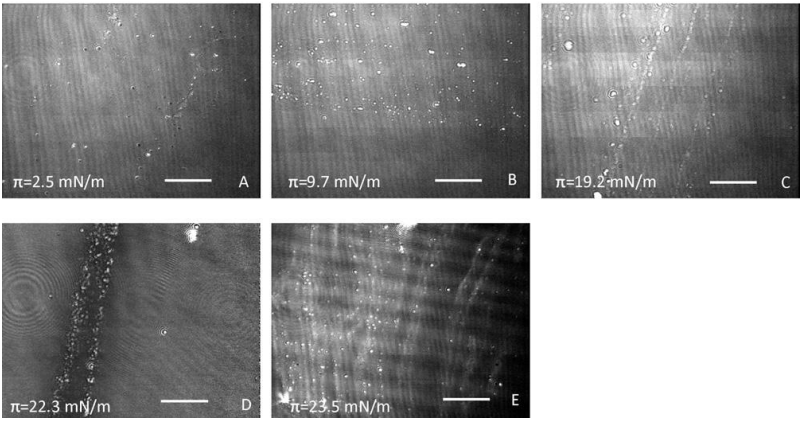

[Appendix 9] BAM images of human serum albumin (HSA) at different surface pressure. The scale bar is 20 µm. A: very small bright circular domains begin to be formed at low surface pressure when compressed. B: They grow in number because of the compression. C: The circular domains are grouping in rows when the monolayer becomes close to the coiled state ("loops"). D and E: The domains merge together to create thick bright fringes, which are attributed to the packing of the "loops", along the pseudoplateu of monolayer isotherm (Toimil et al, 2012).

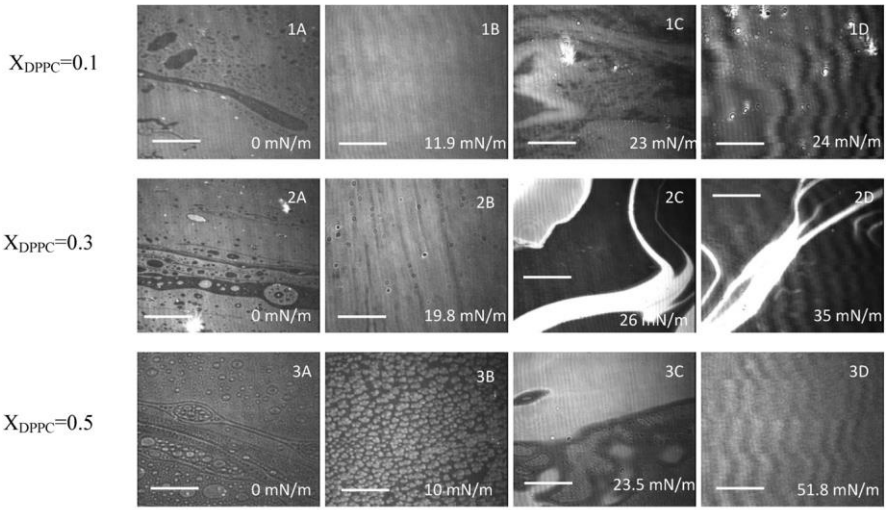

[Appendix 10] BAM images of pure 1,2-dipalmitoyl-sn-glycero-3-phosphocholine (DPPC) and of HSA/DPPC mixture monolayer with different fraction of DPPC at different surface pressure. Zone A: G/LE phase transition of lipids; Zone B: between the LE/C phase transition of DPPC monolayer and the formation of protein "loops" at the interface; Zone C: the exclusion of proteins; Zone D: the collapse of monolayer. Image 1B: a homogeneous protein monolayer in the unfolded state; 2B; "bands" of different reflectivity when the protein changes into "loops" conformation at the interface; 1C and 3C: thick fringes because of protein packed "loops" separated from homogeneous C phase of lipid monolayer (immiscibility) ; 2C and 2D: large domains of collapsed protein, which is separated by lipid condensed state (Toimil et al, 2012).

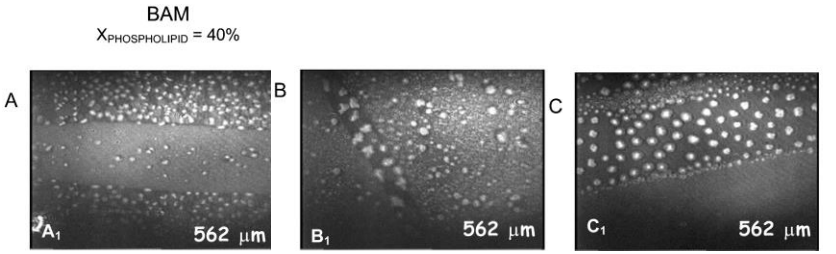

[Appendix 11] BAM images of DPPC/b-casein mixture monolayer at surface pressure below that for b-casein collapse. These BAM images display two distinct regions (a homogeneous bright region – protein and irregular liquid condensed domains – lipid). A1 and B1: both regions are miscible at pH 5 and 7 each; C1: Two regions are clearly separated and immiscible (Caro et al., 2005).

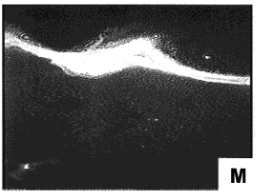

[Appendix 12] BAM images of monopalmitin/whey protein isolate (WPI) mixture monolayer. A Collapsed WPI region at highest pressure. The images are 630 μm× 470 μm (Rodríguez Patino et al., 2001).